Broad spectrum detection of DNA damage by Repair Assisted Damage Detection (RADD)

Nathaniel W.Holton[a], YuvalEbenstein[b], Natalie R.Gassman[a]

[a] Department of Oncologic Sciences, University of South Alabama Mitchell Cancer Institute, Mobile, AL, 36604, USA

[b] School of Chemistry, Center for Nanoscience and Nanotechnology, Center for Light-Matter Interaction, Raymond and Beverly Sackler Faculty of Exact Sciences, Tel Aviv University, Tel Aviv, Israel

Abstract

Environmental exposures, reactive by-products of cellular metabolism, and spontaneous deamination events result in a spectrum of DNA adducts that if un-repaired threaten genomic integrity by inducing mutations, increasing instability, and contributing to the initiation and progression of cancer. Assessment of DNA adducts in cells and tissues is critical for genotoxic and carcinogenic evaluation of chemical exposure and may provide insight into the etiology of cancer. Numerous methods to characterize the formation of DNA adducts and their retention for risk assessment have been developed. However, there are still significant drawbacks to the implementation and wide-spread use of these methods, because they often require a substantial amount of biological sample, highly specialized expertise and equipment, and depending on technique, may be limited to the detection and quantification of only a handful of DNA adducts at a time. There is a pressing need for high throughput, easy to implement assays that can assess a broad spectrum of DNA lesions, allowing for faster evaluation of chemical exposures and assessment of the retention of adducts in biological samples. Here, we describe a new methodology, Repair Assisted Damage Detection (RADD), which utilizes a DNA damage processing repair enzyme cocktail to detect and modify sites of DNA damage for a subsequent gap filling reaction that labels the DNA damage sites. This ability to detect and label a broad spectrum of DNA lesions within cells, offers a novel and easy to use tool for assessing levels of DNA damage in cells that have been exposed to environmental agents or have natural variations in DNA repair capacity.

Graphical abstract

The Repair Assisted Damage Detection assay is a modular cell based assay for the detection of basal DNA damage and DNA damage induced by exogenous exposures.

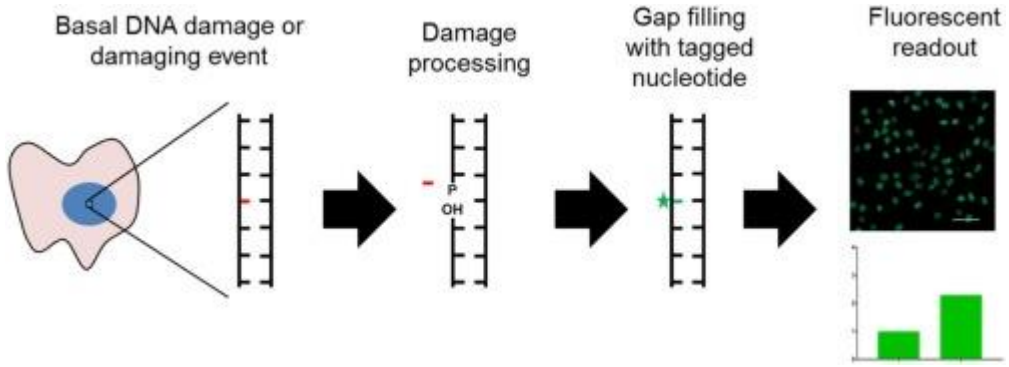

Abbreviations

RADD, repair assisted DNA damage detection; TUNEL, Terminal deoxynucleotidyl transferase nick end labeling; ISEL, In situ end label; DDR, DNA damage response; TdT, terminal deoxynucleotidyl transferase; dUTP, deoxyuracil triphosphate; CSK, cytoskeletal buffer; CPD, cyclyobutane pyrimidine dimer; BrdU, bromodeoxyuridine.

Keywords

DNA damage detection; DNA repair; DNA adduct; Fluorescence; Confocal microscopy

1. Introduction

Nucleic acids are continuously subjected to modification by endogenous and exogenous sources. The formation and retention of these nucleic acid modifications or adducts can threaten the fidelity of the genome by altering the nucleic acid structure, changing base pairing and promoting the likelihood of insertions, deletions and translocations. Detection and removal of DNA damage is essential for maintaining genomic integrity and a tailored and lesion specific DNA damage response (DDR) has evolved for signaling the enzymatic recognition of DNA adducts and corrdinating repair by a suite of DNA repair pathways. Mutations in genes involved in DNA repair are linked to aging and genetic diseases, as well as cancer predisposition, and these mutations can also alter treatment outcomes [[1], [2], [3], [4]]. Therefore, assessment of DNA damage formation and persistence in cells aids in the determination of the genotoxic or carcinogenic potential of chemical or environmental exposures and may identify subpopulations vulnerable to exposure effects. This potential has led to the development of assays that monitor and measure the formation and retention of DNA adducts within a genome, in order to assess the functional DNA repair capacity (reviewed in [[5], [6], [7]]).

Liquid chromatography and mass spectrometry have been used extensively to identify and quantify DNA adducts. These methods have allowed precise quantitation of adduct levels in purified DNA samples and have significantly advanced our understanding of the structure and lifetime of DNA adducts. However, these techniques require expert users, expensive equipment, often employ isotopic labeling for precise quantitation, and require microgram quantities of isolated DNA [6,8,9]. While there are distinct advantages to utilizing these techniques to measure specific adducts, there are issues with DNA isolation procedures introducing further DNA damage and in the standardization of measurements [10].

More accessible forms of DNA damage and adduct detection are antibody based strategies, comet assays, and enzymatic detection by terminal deoxynucleotidyl transferase (TdT). Antibody strategies can be applied to isolated DNA, in cells, or in fixed tissues. While antibodies exist for strand break signals (γH2AX or 53BP-1) and some DNA lesions (6-4 photoproducts, cyclobutane pyrimidine dimers (CPD), etc.), these techniques are limited by the variation and specificity of available antibodies and may be difficult to multiplex due to incompatibilities in fixation or staining procedures. Comet assay or Single Cell Gel Electrophoresis allows more specific strand break detection in cells, eliminating the requirements for specific antibodies, and with modifications can detect alkali labile sites, oxidative base damage, and DNA cross-linking [11,12]. However, comet assay has been

difficult to standardize and reproduce from lab to lab, though comet chip technologies and automated image processes are improving these shortcomings [[13], [14], [15]].

Terminal deoxynucleotidyl transferase dUTP nick end labeling (TUNEL) and in situ (DNA) end labeling (ISEL) [[16], [17], [18]] have also been employed extensively over the past 20 years to detect DNA strand breaks during apoptosis and in some cases DNA damage across a variety of biological samples [[19], [20], [21]]. However, just like the other methods, there are drawbacks to using TUNEL or ISEL because they are highly specific for 3′-OH ends. Several TUNEL modifications have emerged extending its ability to detect other types DNA ends (i.e., 3′-PO_4) or improve DNA damage detection by incorporating FPG to excise oxidative DNA adducts [22].

While all of these techniques are used extensively in the literature to assess DNA damage and adduct formation, each has significant limitations for broad spectrum detection of DNA damage. This gap in methodologies has led us to develop the Repair Assisted Damage Detection (RADD) assay, which harness the action of specific DNA repair enzymes to recognize and excise DNA adducts throughout the genome. Once the DNA adduct has been removed, the adduct position is tagged by insertion of a biotinylated deoxyuridine triphosphate (dUTP). This method has proven viable for detecting DNA lesions on isolated DNA [23], and here we demonstrate for the first time that this detection scheme can be extended to fixed cells to measure DNA damage *in situ*.

The assay provides a novel platform for the characterization of nuclear DNA damage within and across different cell lines by scoring the DNA lesion load. The experiments outlined herein demonstrate that RADD is a robust and novel assay for the measure of nuclear DNA damage and has the potential to be used to investigate specific DNA repair mechanisms, to address risk assessment for both environmental toxicology and cancer etiology, and to evaluate DNA targeted cancer therapies.

2. Material and methods

2.1. Cell culture

A375P cells were purchased from the American Type Culture Collection (ATCC CRL-3224) and maintained in Dulbecco's modified Eagle's medium (DMEM) high glucose (Hyclone #SH30022.01) and supplemented with 10% fetal bovine serum (Atlanta Biologicals # S11550) and 1% sodium pyruvate (Gibco # 11360-070). Chinese hamster ovary (CHO-K1) cells were received from Dr. Samuel H. Wilson at the National Institute of Environmental Health Sciences and grown in minimal essential medium (MEM, Hyclone #SH30265FS) supplemented with 10% FBS. All cells were maintained in a 5% CO_2 incubator at 37 °C and fewer than 10 cell passages were utilized experimentally. Mycoplasma testing was regularly performed using Lonza MycoAlert® and no contamination was detected.

2.2. Cytotoxicity

Cytotoxicity was determined by growth inhibition assay. A375P cells were plated at a density of 4×10^4 cells per well in a 6-well plate (Greiner Bio-One #657165) or 35 mm dish (Falcon #353001) and treated the following day. Prior to DNA damage the cells are washed with Dulbecco's phosphate buffered saline (PBS, Cellgro #21-031-CV) or Hanks' balanced salt solution (HBSS, Hyclone #SH30031.02) for UV and $KBrO_3$ damage, respectively. Cells

were either exposed to a specified dose of UVC (254 nm) using the Spectroline® Spectrolinker XL-1000, or exposed to potassium bromate ($KBrO_3$, Sigma Aldrich #309087) diluted in media for 1 h. Following the damage induction cells were washed one time in HBSS, and growth media was replaced. Cells were maintained in a 5% CO_2 incubator at 37 °C until untreated control cells reached approximately 90% confluency, typically 4-5 days. The cells were then briefly treated with 0.25% Trypsin (Life technologies #25200-056), resuspended in 1 mL of PBS, and counted with Bio-Rad TC20 automated cell counter. Results are presented as the ratio of the number of cells in treated well to cells in control well (% control survival) with error bars representing the standard error of the mean (SEM).

2.3. Repair Assisted Damage Detection

A375P cells were plated at 2.5×10^6 in a 6-well plate with coverslips (VWR #48366-227) or 35 mm glass fluorodishes (World Precision Instruments #FD35-100). The following day the DNA damage was induced as described in the cytotoxicity methods with the UV and $KBrO_3$ doses indicated, and cells were either immediately processed for damage detection or allowed to repair for the indicated times. At the indicated time, cells were washed twice with PBS and incubated with cytoskeletal buffer (CSK, 100 mM NaCl (Fisher Scientific #7647-14-5), 300 mM sucrose (VWR #0335-1KG), 10 mM PIPES pH 6.8 (Amresco #108321-27-3), 3 mM $MgCl_2$ (Amresco #7786-30-3), 0.5% Triton X-100 (Sigma-Aldrich #T8787)) on ice for 5 min, followed by three washes with PBS. The samples were then incubated with 2% formaldehyde (Amresco #M134) in PBS for 10 min at room temperature (~23° C) and washed three times with PBS. They were next treated with 0.25% Triton X-100 (Sigma-Aldrich #T8787) in PBS for 10 min again at room temperature and washed twice with PBS, followed by one wash with sterile deionized H_2O. The DNA damage processing mix contains enzymes purchased from NEB (UDG #M0280S, Fapy-DNA glycosylase # M0240S, T4PDG #M0308S, Endo IV # M0304S, Endo VIII # M0299S) and prepared in 1 x Thermpol buffer (NEB # B9004S) and incubated at 37 °C in a humidified incubator for one hour. Next, the gap filling mix, again prepared in 1 x Thermpol buffer, is added to the DNA damage processing mix, and incubated for an additional hour at 37° C. The RADD enzymes and their functions are outlined in Table 1 and the sequential DNA damage processing and gap filling reactions are outlined in Table 2. The enzyme cocktails were then washed with 1% bovine serum albumin (BSA, Jackson ImmunoResearch # 001-000-162) in PBS three times and blocked with 5% goat serum (Invitrogen #31873) in PBS for 30 min at room temperature. The blocking serum was then aspirated, and the goat anti-biotin FITC conjugated antibody (Sigma-Aldrich #F6762) is diluted 1:400 in 5% goat serum in PBS and incubated at room temperature for 1 h, protected from light. The cells were washed three times with 1% BSA (Jackson ImmunoReseach #001-000-162) in PBS, dried briefly, and mounted in Prolong® Gold with DAPI (Life Technologies #P36931) following the manufacturer's instructions.

Table 1. **RADD assay enzymes.** The RADD assay utilizes the action of several glycosylases and endonucleases that recognize and process a broad spectrum of DNA lesions to create an appropriate substrate to be filled by DNA polymerase. The DNA end chemistry after RADD enzymatic processing is provided for both the 5′ and 3′ termini, P (phosphate), P-dimer (phosphate with covalently bound pyrimidine attached), P-UA (3′-phospho-α,β-unsaturated aldehyde), dRP (5′-deoxyribose-5-phosphate), OH (hydroxyl).

The DNA polymerase I Klenow large fragment is utilized to incorporate biotinylated dUTP at sites of DNA damage.

Enzyme	Substrate Specificity	Processed terminal ends 5′ 3′	
Uracil DNA glycosylase	uracil	AP site	
Formamidopyrimidine [Fapy]-DNA glycosylase	7, 8-dihydro-8-oxoguanine (8-oxoguanine), 8-oxoadenine, fapy-guanine, methy-fapy-guanine, fapy-adenine, aflatoxin B1-fapy-guanine, 5-hydroxy-cytosine and 5-hydroxy-uracil	P	P
T4 Pyrimidine dimer glycosylase	cis-syn-cyclobutane pyrimidine dimers and AP sites	P-dimer	P-UA
Endonuclease IV	AP sites and diesterease activity modifies 3′ phosphates	dRP	OH
Endonuclease VIII	urea, 5, 6- dihydroxythymine, thymine glycol, 5-hydroxy-5-methylhydanton, uracil glycol, 6-hydroxy-5, 6-dihydrothymine and methyltartronylurea	P	P
Klenow DNA polymerase large fragment	Incorporates modified dUTPs at sites of DNA damage created by the damage processing enzymes	DNA synthesis 5′ to 3′	

Table 2. **RADD sequential reaction conditions**. RADD is performed in two sequential reactions without aspirating reagents between reactions. The DNA damage processing mix (left) is placed on fixed and permeabilized cells and placed in a humidified incubator. The gap filling mix (right) is added directly to the lesion processing mix and incubated for an additional hour. The reagents are then aspirated and the cells are washed and incubated with anti-biotin FITC conjugated antibody.

Lesion processing mix	100 µL total reaction volume	Gap filling mix	50 µL total reaction volume
UDG	2.5 U	Large (Klenow) Fragment DNA pol I	5 U
FPG	4 U	Biotin-11-dUTP	1 µM
T4 PDG	5 U	10 X Thermpol buffer	5 µL
Endo IV	5 U		
ENDO VIII	5 U		
NAD+	500 µM		
BSA	200 µg/mL		
10 X Thermpol buffer	10 µL		

2.4. Laser micro-irradiation

Laser micro-irradiation was performed as previously described [24]. Briefly, CHO-K1 cells were plated at 3×10^4 cells per chamber in an 8 chamber slide (Nunc LabTek II, ThermoFisher # 12-565-338) and sensitized with 10 µM bromodeoxyuridine (BrdU, Sigma Aldrich #B5002) for 24 h prior to micro-irradiation. During micro-irradiation, cells were placed in a microscope stage incubator and maintained at 37° C with 5% CO_2. A 405 nm

laser (Coherent Obis) coupled to a Nikon A1rsi laser scanning confocal microscope was used to induce DNA damage by creating a damage region of interest (ROI) consisting of a 3 × 3 pixel area that was stimulated at 0.5 frames per second (fps) through a 20 x C-Apochromat (NA 0.75) dry objective. The post objective laser output was measured to be 2.4 mW using a PM100D power meter equipped with a S170C objective plane power sensor (THORLabs #S170C and S150C) and 0.5 fps stimulation.

2.5. Immunofluorescence

Following micro-irradiation cells were fixed and permeabilized in 100% ice cold methanol for 15 min followed by 5 washes with PBS to allow cells to fully rehydrate. Prior to probing for the DNA strand break proteins cells were blocked in 1% BSA in PBS for 30 min at room temperature. Cells were then incubated with the primary antibodies for γH2AX (Millipore 05-363) and XRCC1 (abcam ab1838) diluted in 1% BSA in PBS at a 1:750 and a 1:50 respectively for 1 h at room temperature. For the cyclobutane pyrimidine dimer (CPD) immunofluorescence, cells were fixed and rehydrated as described, and then the DNA was denatured using 2N hydrochloric acid (HCl, Fisher #SA49) for 45 min at room temperature and washed 5 times with PBS. Samples are then neutralized in 50 mM Tris-HCl pH 8.8 (Amresco #J383) for 5 min at room temperature and washed 3 times with PBS. Samples are blocked in 5% normal goat serum (Pierce #31873) for 30 min at room temperature followed by an incubation with anti-CPD (Cosmo Bio clone TDM2) in 5% goat serum for 1 h at room temperature. All samples were then washed 3 times with PBS and incubated with Alexa-488 goat anti-mouse (ThermoFisher #A11034) in 1% BSA for 1 h at room temperature protected from light. Samples were washed 3 times with PBS and the nucleus was stained using NucBlue® fixed cell stain (DAPI, ThermoFisher #R37606) following the manufacturer's instructions.

2.6. Imaging and image analysis

Fluorescence images were acquired using the Nikon A1rsi laser scanning confocal microscope using a 20 x dry objective (numerical aperture 0.75). Multi-channel configuration was used to ensure the absence of excitation cross-talk or emission bleed-through between channels. The gain of the 405 nm laser line was set so the nucleus is clearly defined following DAPI staining. To image the DNA damage sites labeled with the FITC-anti-biotin antibody (RADD signal), the 488 nm laser gain was set to 2.5 for all quantitative imaging acquisition. The gain setting was determined by first examining cells processed with both the DNA damage and gap filling mixes, though the Klenow was omitted from the gap-filling step. Imaging of the no Klenow processed cells reveals a low level of non-specific staining in the cytoplasm and no nuclear staining (Supplemental Fig. 2), and the gain was set to eliminate this non-specific signal. We have previously employed this method to address non-specific antibody staining for signal quantitation [25]. Then the untreated, but completely processed control cells were examined and gain was adjusted to image their relative intensity to above the background. These imaging procedures eliminate the presence of non-specific antibody staining, while allowing the basal levels of DNA damage to be detected in the untreated cells.

2-D images were acquired, and DAPI staining was used to select the largest cross section of the nucleus for imaging. Images were acquired with a pinhole of 3 airy units (AU) and a zoom of 1.0. NIS-Elements AR 4.51 software was used for all image acquisition.

Image analysis was performed using the Fiji ImageJ software package (https://fiji.sc/). Images were cropped to eliminate partial cells on the borders and cells not in the focal plane. Images were not cropped more than 30% of the original picture size 512 × 512. The RADD signal was scored using the DAPI channel to define the nucleus and applying that mask to the FITC channel in order to measure the mean nuclear signal intensity of the anti-biotin-FITC conjugated antibody in the nucleus. A minimum threshold was applied to select nuclei, and analyze particles was used to filter nuclei sizes between 50 and 1000 μm to prevent large aggregates from being analyzed. Representative images are shown, and graphs were constructed from measuring the nuclear fluorescence intensity across multiple image fields from independent treatment events ($n \geq 3$). The statistical significance was calculated by averaging the mean fluorescence intensity per nuclear area for all the cells of a particular treatment, when comparing two damaging agents values were normalized across experiments to the untreated cells. The *p*-values were calculated using ANOVA or an unpaired *t*-test as appropriate and the significance is listed for each experiment compared to untreated cells with * = $p < 0.05$, ** = $p < 0.01$, *** = $p < 0.001$.

3. Results

3.1. RADD theory and reaction components

The RADD assay was designed as an adaptable assay to characterize a broad spectrum of DNA adducts in fixed cells. Permeabilization allows the RADD enzymes access to the nucleus in order to process the DNA lesions present in the nuclear DNA. DNA lesions are first processed by a well characterized suite of DNA repair enzymes, and the resulting gaps are then filled with a biotinylated nucleotide to allow for the DNA damage to be scored by fluorescence microscopy (Fig. 1).

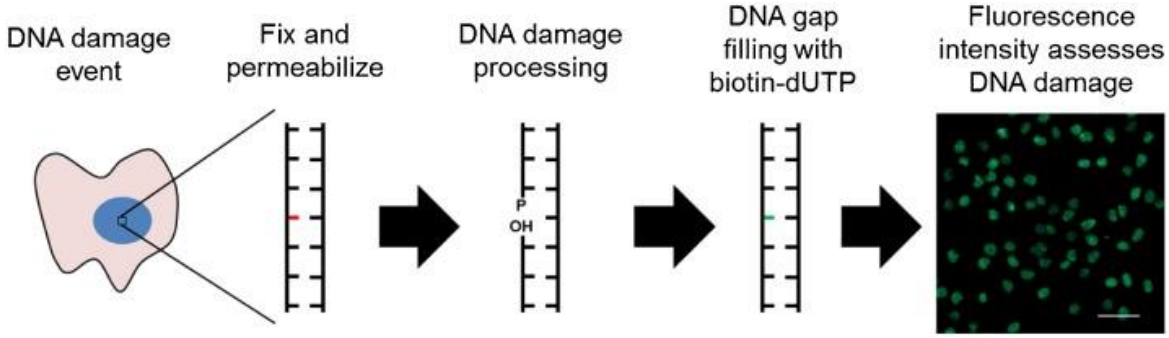

Fig. 1. **RADD workflow diagram.** RADD workflow diagram beginning with a damage event or endogenous basal DNA damage followed by fixation and permeabilization. Cells are then incubated with DNA damage processing mix (UDG, FPG, T4PDG, Endo IV, Endo VIII), followed by co-incubation with the DNA gap filling mix (Klenow DNA polymerase, biotin-dUTP). Cells are visualized after incubation with anti-biotin-FITC conjugated antibody and fluorescence confocal microscopy (scale bar = 50 μm).

The RADD assay utilizes repair enzymes that are bacterial in origin and are capable of recognizing various oxidized bases, the modified base uracil, pyrimidine dimers, and 6-4

photoproducts (Table 1). Uracil DNA glycosylase (UDG), Fapy-DNA glycosylase (FPG), T4 pyrimidine dimer glycosylase (T4 PDG), and Endonuclease VIII (Endo VIII) recognize and process a large cross section of DNA adducts found in cells; however, the processed DNA ends are not always compatible for DNA synthesis. For the RADD reaction to successfully label these sites of DNA damage, further processing by Endonuclease IV (Endo IV) is needed to create the appropriate 3′ hydroxyl group required for the subsequent gap filling reaction.

Endo IV has two important functions in the DNA damage processing mix of the RADD assay. First, the enzyme processes apurinic/apyrimidinic (AP) sites to create the appropriate DNA end chemistry. Second, Endo IV has diesterease activity that modifies the 3′ phosphates created by the other RADD enzymes to hydroxyl groups. The large fragment of Klenow DNA polymerase, which lacks the 5′ to 3′ proofreading activity, is then used to incorporate biotinylated dUTP at the processed damage sites created by the DNA damage processing reaction (Table 2). The biotinylated nucleotide provides a trackable substrate when incubated with anti-biotin FITC-conjugated antibody. The resulting biotin-dUTP repaired cells can be scored for the relative fluorescence intensity in the nucleus, which provides a measure of the DNA damage lesion load, repair efficiency and overall damage response of the cell population.

3.2. Disrupting the cytoplasm increases the nuclear RADD signal

In order to efficiently detect DNA lesions in cells, the RADD assay requires that the enzymatic load of the DNA damage processing and gap filling reaction cocktails reach the nucleus and act on exposed DNA lesions. Several permeabilization techniques were investigated in a number of cell lines to optimize the nuclear fluorescence signal of RADD. The melanoma cell line, A375P, was the most difficult to permeabilize and detect damage in, so it is the model cell line used in the optimization work. Standard permeabilization techniques with both ice cold methanol and 0.25% Triton X-100 allowed for some detection of DNA lesions within the nucleus, but the signal was low in the nuclear compartment, and many cells accumulate a halo surrounding the nuclear envelope (Fig. 2). However, cells that are treated with CSK, a hypotonic solution, followed by mild permeabilization prior to RADD contained a much more uniform and robust nuclear fluorescence signal (Fig. 2). Treatment of cells with CSK buffer removes much of the cytoplasm and likely allows the RADD enzymes a less encumbered route when diffusing into the nucleus. The fixation, permeabilization, and use of CSK treatment must be evaluated and optimized for each cell line to produce a robust RADD signal above background.

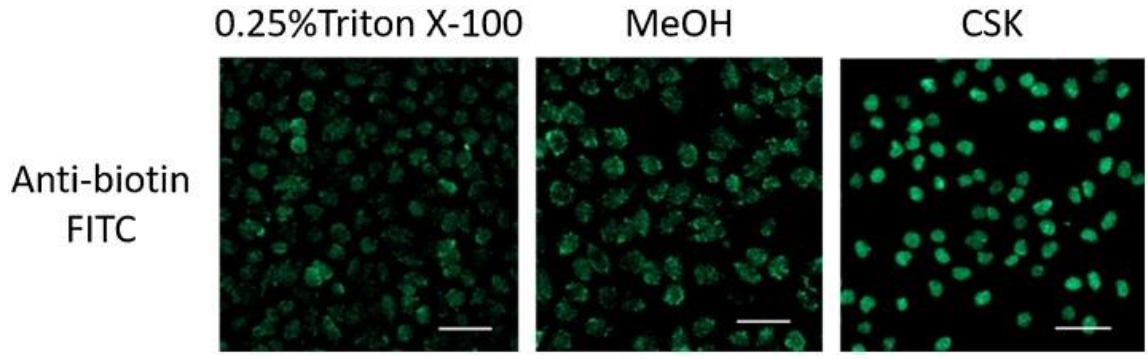

Fig. 2. **Whole cell RADD signal is increased by treatment with CSK buffer.** A375P cells were fixed and permeablized using three different methods followed by RADD assay readout. The panel of confocal images are representative of undamaged A375P melanoma cells (scale bar = 50 μm).

3.3. RADD detects lesions induced by oxidizing agents and UV

In order to validate detection of induced DNA damage and assess the sensitivity of the assay, cells were expose to two common environmental damaging agents prior to RADD analysis. DNA damage was induced in A375P cells by exposing them to the oxidizing agent $KBrO_3$ or to UVC light. Sensitivity of the A375P cell line to these agents was first characterized by cell growth inhibition. $KBrO_3$ induced cell death in the mM range, with near complete cell growth inhibition at concentrations greater than 30 mM (Fig. 3A). UVC exposure fully inhibited cell growth at doses above 60 J/m^2 (Fig. 3B).

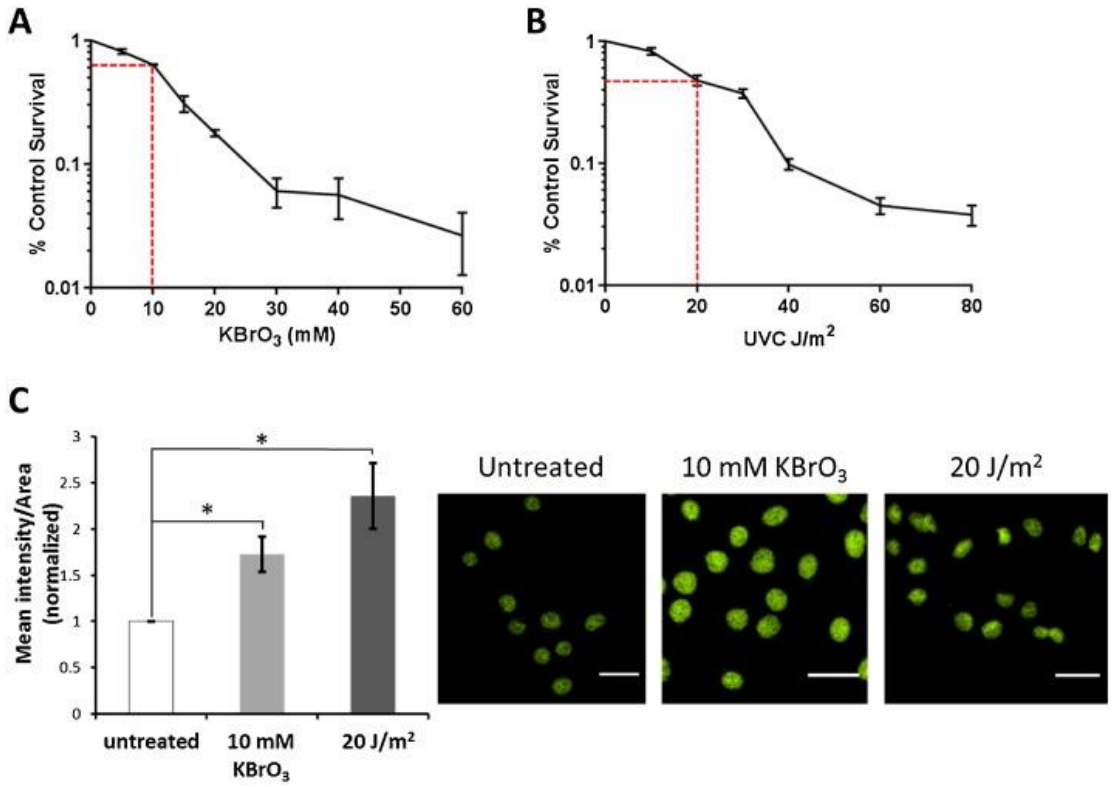

Fig. 3. **RADD can detect UVC and $KBrO_3$ induced DNA damage.** (A and B) A375P cells were treated with increasing doses of $KBrO_3$ (1 h) or UVC and grown until control, untreated cells reached approximately 95% confluency. Graphs are representative of the percent survival relative to the untreated control. (C) A375P cells were treated with sub-lethal doses of UVC and $KBrO_3$ and the RADD assay was performed to detect DNA lesions normalized to the undamaged control. Image panels are representative of cells quantified to create the graph. All graphs were constructed from three independent experiments with error bars representing the SEM and * indicates $p < 0.05$ relative to untreated cells (scale bar = 25 μm).

Based on the cell sensitivity curves, the doses of 10 mM $KBrO_3$ (64% cell survival) and 20 J/m^2 UVC (48% cell survival) were used to validate the ability of RADD to detect DNA damage created by these treatments. Verification of the induction of DNA adducts by $KBrO_3$ and UV treatment was confirmed by slot blot analysis of the genomic DNA

(Supplemental Fig. 1). RADD was able to detect the induced DNA damage created by both treatments with relative fluorescence signal intensities of 1.7X and 2.3X above untreated cells for $KBrO_3$ and UV induced damage, respectively. This demonstrates that RADD is capable of detecting, not only the basal levels of DNA damage in the cells, but also the induction of nuclear DNA damage in the forms of oxidized bases, such as 8-oxo-2′-deoxyguanosine (8-oxodG), created by 10 mM $KBrO_3$ treatment for 1 h, as well as UV induced bulky adducts, such as CPD.

Repair of these lesions can also be monitored by performing a RADD time course after damage induction and monitoring the changes in fluorescent signal as a function of time (Fig. 4). A375P cells were treated with 10 mM $KBrO_3$ for 1 h, then RADD was performed after allowing cells to repair for 4, 12, and 24 h. RADD was able to detect not only the induction of lesions (0 time point), but also show their removal as a function of repair time, demonstrated by the reduction in fluorescence signal over the time course. The selected dose of 10 mM $KBrO_3$ is mildly cytotoxic to the A375P cells, so return to basal levels of DNA damage after 24 h is consistent with cells surviving the induced DNA damage.

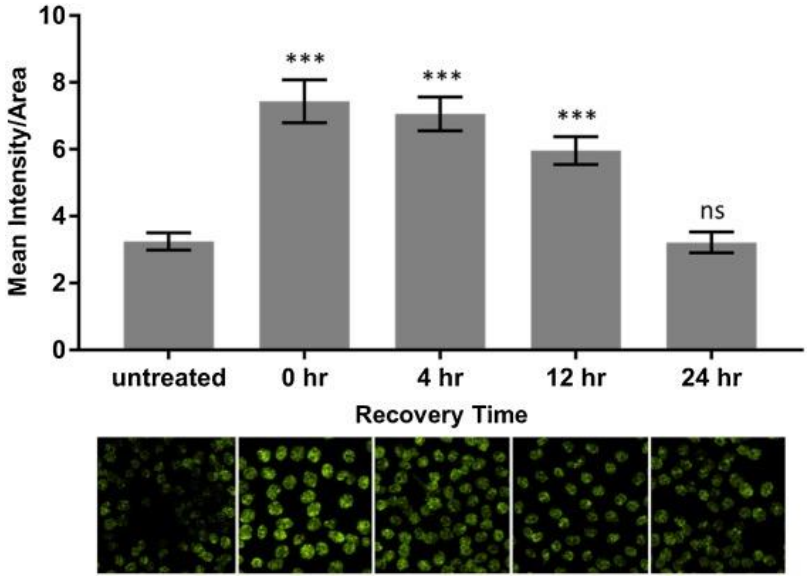

Fig. 4. **RADD detection of $KBrO_3$ induced lesions over time.** RADD assay was performed on A375P cells treated with 10 mM $KBrO_3$ for 1 h, and then allowed to recover for the indicated time points. Graphs were constructed from more than 350 cells per time point and error bars represent the SEM with *** indicating $p < 0.001$ relative to untreated cells. Images are representative each time point that was analyzed by RADD.

3.4. RADD detects the base lesion BrdU and DNA damage induced by laser micro-irradiation

Laser micro-irradiation has emerged as a powerful and commonly used tool to characterize the DDR following a sub-nuclear dose of laser irradiation. DNA repair has been investigated by micro-irradiation at wavelengths ranging from UV to near infra-red, with most wavelengths inducing mixtures of base damage and single and double strand DNA breaks [26,27]. The use of sensitizing agents like BrdU has been employed to reduce the dose of laser irradiation needed to elicit a DDR. BrdU is a modified nucleotide that is an analog of thymidine and is inserted into the DNA of actively replicating cells. The increase in

sensitization is the result of the BrdU being spontaneously liberated from the DNA backbone by UVB or UVA excitation, producing an abasic site [28]. Additionally, specific laser wavelengths have also been shown to produce reactive oxygen species when interacting with BrdU moieties to produce oxidative damage in addition to the base loss. To examine if the RADD assay could detect the incorporation of BrdU and detect the DNA damage site created by laser micro-irradiation, we employed the CHO-K1 cells, for which we have previously characterized the laser micro-irradiation damage response [24].

CHO-K1 cells were first sensitized for 24 h with BrdU and incorporation of BrdU into the genomic DNA was probed using RADD. As shown in Fig. 5A, basal levels of DNA damage in the CHO-K1 cells were detected using RADD, and cells exposed to BrdU showed increased levels of DNA lesions as detected by the increase in mean fluorescence intensity of the nucleus.

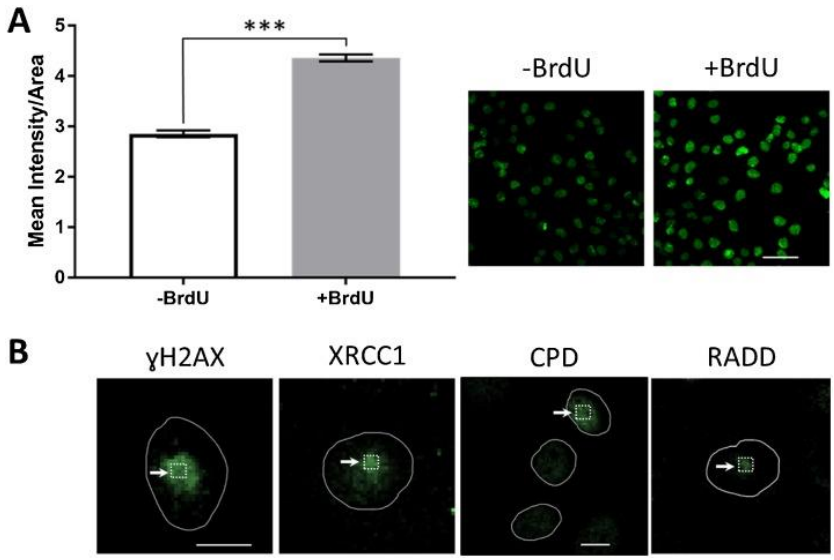

Fig. 5. **RADD can detect BrdU incorporation and DNA damage induced by laser micro-irradiation.** (A) CHO cells were sensitized with 10 μM BrdU for 24 and BrdU incorporation was detected by RADD. The bar graph was constructed by measuring the nuclear intensity per area of 4 independent BrdU sensitization events with representative images adjacentThe error bars represent the SEM of all the cells measured and *** indicates $p < 0.001$ relative to untreated cells. (B) Laser micro-irradiation was performed on CHO cells that were sensitized with 10 μM BrdU for 24 h. Cells were fixed 5 min post irradiation with the 405 nm laser stimulation (2.4 mW) and probed with monoclonal antibodies or RADD. Scale bar represents 10 μm.

Laser micro-irradiation was then used to induce DNA damage in these cells. Laser-induced DNA damage is often characterized by observing the recruitment and retention of DNA repair proteins to the site of induced damage, via fluorescently-tagging or immunofluorescence, and the types of DNA damage induced are often characterized by immunofluorescent detection of strand break markers, such as XRCC1, γH2AX or 53BP-1, or adducts, such as 8-oxodG, CPD, or 6-4 photoproducts. Here, we utilized the RADD assay to detect the induction of DNA damage in the CHO-K1 cells 5 min post micro-irradiation, and compared the RADD detected spot to the commonly used strand break and damage markers.

CHO-K1 cells irradiated at 0.5 fps show a large γH2AX foci that covers much of the nucleus, showing signal propagation from the site of induced damage (Fig. 5B). The single strand break and base excision repair protein XRCC1 also showed recruitment to the induced damage site, and while distinct foci did form, the signal was still diffuse (Fig. 5B). When the RADD assay was performed on cells that were micro-irradiated, the localization of the fluorescent signal was tightly correlated with the damage ROI used to create the laser induced DNA damage. Further, the RADD detected signal was also significantly better than the lesion detection antibody for CPD, which required denaturing of the DNA to generate the diffuse spot observed (Fig. 5B).

Overall, the RADD assay has the ability to characterize the damage created by the modified DNA base used to sensitize the reaction and the laser micro-irradiation itself. It provides a distinct advantage over adduct antibodies, which may perform poorly and require DNA to be denatured for recognition, and strand break signals, like γH2AX, which has been shown to develop in the absence of detectable DSBs or develop pan-nuclear signaling making break sites difficult to detect [29,30].

4. Discussion

The dynamic nature of DNA damage and repair requires creative methods to characterize, quantify, and localize DNA adducts. New methodologies are needed to bridge the gap between detecting single DNA adducts with extreme precision and detecting large numbers of adducts in a single method. As demonstrated here the RADD assay provides a dynamic, simple and accessible technique to assess a broad spectrum of DNA adducts in a cellular context over time and is capable of measuring global nuclear DNA damage (UVC, $KBrO_3$, and BrdU) and sub-nuclear laser micro-irradiation induced damage with a more focused signal generation than commonly used antibody detection techniques.

Detections and quantification of DNA adducts is still technically challenging because of the large variety of DNA adducts are generated by endogenous and exogenous exposures. The use of enzyme cocktails to detect, excise, or tailor DNA ends to improve the detection of DNA damage is not a new concept. Fpg, T4 PDG, and similar enzymes have been utilized in the comet assay to improve the detection of alkali labile sites, oxidative base damage, and DNA cross-linking [11,12]. Similarly, enzyme cocktails have be used to develop modifications of the commonly used TUNEL assay to improve its detection of DNA damage [22]. Yet, these modified assays are not commonly used in the assessment or quantification of DNA damage. Whether this is due to difficulty in implementation or the need for specialized equipment is unclear.

Given the limited adoption of these assays for lesion detection and the fundamental limitations of antibody detection strategies, we have sought to develop an assay that address the fundamental need to detect and provide relative quantification of DNA adducts and DNA damage. RADD utilizes an easy to implement enzymatic and immunofluorescence strategy that can be adopted by any laboratory and integrated into existing experimental pipelines. From fixation to imaging, the assay can be performed within 4 h, comparable with processing and preparation times for existing TUNEL and immunofluorescence protocols, and is scalable to any size desired by the user.

Previously, an enzymatic cocktail, PreCR® was used to detect, excise, and label DNA adducts with an ATTO-conjugated dUTP on isolated DNA [23]. The optimized cell based RADD assay described here is a logical extension of this previous work with necessary modifications to improve the detection, excision, and labeling of DNA lesions within the cell. In cells, assays like TUNEL have been found to underestimate DNA damage due to chromatin compaction, and DNA repair enzymes have been shown to have difficulty acting on lesions that are found tightly bound by chromatin [31]. To address these difficulties, stronger permeabilization and pre-extraction with CSK was employed along with sequential enzyme cocktail additions to improve the penetration and effectiveness of lesion removal in the RADD assay. By first incubating the lesion processing mix with the cells alone followed by co-incubation with the gap filling mix, the time needed for the DNA repair enzymes to diffuse into the nucleus and act on available DNA lesions is provided. Tagging of the DNA lesion site then occurs in a separate reaction after the DNA repair cocktail has provide the necessary substrate for the Klenow polymerase to fill the gap.

This combination of enzymatic processing and tagging was designed allow RADD to address a much wider spectrum of lesions than current adductomic or damage detection techniques and report on the overall damage state of the genome. Precise quantitation of some DNA adducts can be performed by other techniques, but the RADD assay offers facile tuning of the repair cocktail to address specific lesions (including rare adducts) given that there is an available processing enzyme. Additionally, the gap-filling reaction can also be tailored to a user's needs. In the assay described here biotinylated-dUTP was inserted and used for lesion detection however, given the ability of Klenow to insert a number of modified nucleotides, users could likely incorporate any labeled nucleotide of interest, including fluorescently-labeled nucleotides or azide/alkyne click chemistry compatible molecules. This modularity and adaptability makes RADD a powerful tool for use across many model systems, providing a single technique that is capable of characterizing many DNA repair pathways of interest.

5. Conclusion

RADD is able to detect nuclear DNA lesions in cells and can detect damage across species and tissue types. The RADD assay is highly adaptable and includes: (1) a DNA damage processing mix containing DNA repair enzymes that recognize, remove, and modify DNA lesion sites to contain the appropriate DNA end chemistry for gap filling, and (2) a gap filling mix containing a tagged nucleotide to be incorporated for monitoring the processed DNA damage site. The DNA repair enzymes that are utilized by RADD can be adjusted depending on the DNA lesions being investigated and the tagged nucleotide can also be altered depending on the read-out that is desired. The RADD method provides users with a high content screening assay capable of monitoring a broad spectrum of DNA damage with no DNA isolation required.

Acknowledgments

The Gassman lab is supported by start-up funding from the University of South Alabama Mitchell Cancer Institute. The Ebenstein lab acknowledges funding from the BeyondSeq consortium [EC program 63489]. The authors would like to thank Dr. Joel Andrews and the Cellular and Biomolecular Imaging Facility for assistance with confocal microscopy

experiments. This work was supported by R21ES028015 from National Institutes of Health, National Institute of Environmental Health Sciences.

Appendix A. Supplementary data

The following is Supplementary data to this article:

Download Word document (262KB)

References

[1] S. Negrini, V.G. Gorgoulis, T.D. Halazonetis**Genomic instability–an evolving hallmark of cancer,** Nat. Rev. Mol. Cell Biol., 11 (3) (2010), pp. 220-228

[2] K.A. Olaussen, *et al.***DNA repair by ercc1 in non-small-cell lung cancer and cisplatin-based adjuvant chemotherapy**, N. Engl. J. Med., 355 (10) (2006), pp. 983-991

[3] J. de Boer, J.H. Hoeijmakers**Nucleotide excision repair and human syndromes**, Carcinogenesis, 21 (3) (2000), pp. 453-460

[4] M. Akbari, H.E. Krokan**Cytotoxicity and mutagenicity of endogenous DNA base lesions as potential cause of human aging**, Mech. Ageing Dev., 129 (7-8) (2008), pp. 353-365

[5] S. Jalal, J.N. Earley, J.J. Turchi**DNA repair: From genome maintenance to biomarker and therapeutic target**, Clin. Cancer Res., 17 (22) (2011), pp. 6973-6984

[6] S. Balbo, R.J. Turesky, P.W. Villalta**DNA adductomics**, Chem. Res. Toxicol., 27 (3) (2014), pp. 356-366,

[7] G. Figueroa-Gonzalez, C. Perez-Plasencia**Strategies for the evaluation of DNA damage and repair mechanisms in cancer**, Oncol. Lett., 13 (6) (2017), pp. 3982-3988

[8] J. Guo, *et al.***Multiclass carcinogenic DNA adduct quantification in formalin-fixed paraffin-embedded tissues by ultraperformance liquid chromatography-tandem mass spectrometry,** Anal. Chem., 88 (9) (2016), pp. 4780-4787

[9] M. Dizdaroglu, P. Jaruga, H. Rodriguez**Measurement of 8-hydroxy-2'-deoxyguanosine in DNA by high-performance liquid chromatography-mass spectrometry: comparison with measurement by gas chromatography-mass spectrometry,** Nucleic Acids Res., 29 (3) (2001) (p. E12.30413)

[10] A. Valavanidis, T. Vlachogianni, C. Fiotakis**8-hydroxy-2' –deoxyguanosine (8-ohdg): A critical biomarker of oxidative stress and carcinogenesis**, J. Environ. Sci. Health C Environ. Carcinog. Ecotoxicol. Rev., 27 (2) (2009), pp. 120-139

[11] P.L. Olive, J.P. Banáth**The comet assay: a method to measure DNA damage in individual cells**, Nat. Protoc., 1 (1) (2006), pp. 23-29

[12] C.C. Smith, M.R. O'Donovan, E.A. Martin**Hogg1 recognizes oxidative damage using the comet assay with greater specificity than fpg or endoiii**, Mutagenesis, 21 (3) (2006), pp. 185-190

[13] S. Braafladt, V. Reipa, D.H. Atha**The comet assay: automated imaging methods for improved analysis and reproducibility**, Sci. Rep., 6 (2016), p. 32162

[14] A.R. Collins, *et al.***Controlling variation in the comet assay**, Front Genet, 5 (2014), p. 359

[15] A.R. Collins, *et al.***The comet assay: topical issues**, Mutagenesis, 23 (3) (2008), pp. 143-151

[16] V.V. Didenko**In situ labeling of DNA breaks and apoptosis by t7 DNA polymerase**, Methods Mol Biol, 682 (2011), pp. 37-48

[17] P.J. Hornsby, V.V. Didenko**In situ ligation: a decade and a half of experience**, Methods Mol. Biol., 682 (2011), pp. 49-63

[18] D.T. Loo**Tunel assay: an overview of techniques,** Methods Mol. Biol., 203 (2002), pp. 21-30

[19] V.V. Didenko, H. Ngo, D.S. Baskin**Early necrotic DNA degradation: presence of blunt-ended DNA breaks, 3' and 5' overhangs in apoptosis, but only 5' overhangs in early necrosis**, Am. J. Pathol., 162 (5) (2003), pp. 1571-1578

[20] J.H. van Dierendonck**DNA damage detection using DNA polymerase i or its klenow fragment. Applicability, specificity, limitations**, Methods Mol. Biol., 203 (2002), pp. 81-108

[21] Y. Otsuki, Y. Ito**Quantitative differentiation of both free 3' oh and 5' oh DNA ends using terminal transferase-based labeling combined with transmission electron microscopy**, Methods Mol Biol, 203 (2002), pp. 41-54

[22] D.S. Baskin, M.A. Widmayer, M.A. Sharpe**Quantification of dnase type i ends: dnase type ii ends, and modified bases using fluorescently labeled ddutp, terminal deoxynucleotidyl transferase, and formamidopyrimidine-DNA glycosylase,** Biotechniques, 49 (1) (2010), pp. 505-512

[23] S. Zirkin, *et al.***Lighting up individual DNA damage sites by in vitro repair synthesis,** J. Am. Chem. Soc., 136 (21) (2014), pp. 7771-7776

[24] N.W. Holton, J.F. Andrews, N.R. Gassman**Application of laser micro-irradiation for examination of single and double strand break repair in mammalian cells**, J. Vis. Exp. (2017), p. 56265

[25] T.W. Kirby, *et al.***DNA polymerase beta contains a functional nuclear localization signal at its n-terminus,** Nucleic Acids Res., 45 (4) (2017), pp. 1958-1970

[26] C. Lukas, *et al.***Distinct spatiotemporal dynamics of mammalian checkpoint regulators induced by DNA dama,** Nat. Cell Biol., 5 (3) (2003), pp. 255-260

[27] N.R. Gassman, S.H. Wilson**Micro-irradiation tools to visualize base excision repair and single-strand break repair**, DNA Repair (Amst), 31 (2015), pp. 52-63

[28] C.L. Limoli, J.F. Ward**A new method for introducing double-strand breaks into cellular DNA**, Radiat. Res., 134 (2) (1993), pp. 160-169

[29] J.E. Cleaver, L. Feeney, I. Revet**Phosphorylated h2ax is not an unambiguous marker for DNA double-strand breaks**, Cell Cycle, 10 (19) (2011), pp. 3223-3224

[30] P. Rybak, *et al.***Low level phosphorylation of histone h2ax on serine 139 (gammah2ax) is not associated with DNA double-strand breaks,** Oncotarget, 7 (31) (2016), pp. 49574-49587

[31] A. Campalans, *et al.***Interaction with ogg1 is required for efficient recruitment of xrcc1 to base excision repair and maintenance of genetic stability after exposure to oxidative stress**, Mol. Cell. Biol., 35 (9) (2015), pp. 1648-1658